
A data-centric approach to class-specific bias in image data augmentation

Athanasios Angelakis
Amsterdam University Medical Center
University of Amsterdam - Data Science Center
Amsterdam Public Health Research Institute
Amsterdam, Netherlands
a.angelakis@amsterdamumc.nl

Andrey Rass
Den Haag, Netherlands
anvrass@gmail.com

Abstract

Data augmentation (DA) enhances model generalization in computer vision but may introduce biases, impacting class accuracy unevenly. Our study extends this inquiry, examining DA’s class-specific bias across various datasets, including those distinct from ImageNet, through random cropping. We evaluated this phenomenon with ResNet50, EfficientNetV2S, and SWIN ViT, discovering that while residual models showed similar bias effects, Vision Transformers exhibited greater robustness or altered dynamics. This suggests a nuanced approach to model selection, emphasizing bias mitigation. We also refined a ”data augmentation robustness scouting” method to manage DA-induced biases more efficiently, reducing computational demands significantly (training 112 models instead of 1860; a reduction of factor 16.2) while still capturing essential bias trends.

1 Introduction

Machine learning is generally defined as aiming at systems to solve, or ”learn” a particular task or set of tasks (e.g. regression, classification, machine translation, anomaly detection - (Goodfellow, Bengio, and Courville 2016a) based on some training data, allowing computers to assign labels or predict future outcomes without manual programming. A typical case involves a training dataset that is finite, and the system’s parameters are optimized using a technique such as gradient descent, using some performance measure (e.g. ”accuracy”) for evaluation during optimization and on a holdout ”test” set (LeCun et al. 1998; Bishop and Nasrabadi 2006; Shalev-Shwartz and Ben-David 2014; Goodfellow, Bengio, and Courville 2016a).

In particular, computer vision tasks (e.g. image classification) are contemporarily accomplished via deep learning methods (Feng et al. 2019) such as convolutional neural networks (CNNs), which have continuously been held in high regard as the go-to approach to such problems (LeCun, Bengio et al. 1995; LeCun, Kavukcuoglu, and Farabet 2010; Voulodimos et al. 2018), owing to their ability to extract features from data with known grid-like topology, such as images (Goodfellow, Bengio, and Courville 2016b).

Like any other machine learning systems, CNNs can suffer from overfitting - a performance gap between training and test data samples, which represents inability to generalize the learned task to unseen data (Goodfellow, Bengio, and Courville 2016c). To combat this, various regularization methods have been developed for use during optimization (Tikhonov 1943; Tihonov 1963). Particular (though not limited - (Ko et al. 2015)) to image-based tasks is the use of data augmentation - applying certain transformations, such as random cropping, stretching and color jitter, to training data during training iterations. Such techniques are near-ubiquitous in computer vision tasks due to their effectiveness as a regularization measure (Shorten and Khoshgoftaar 2019).

However, recent research by Balestrieri, Bottou, and LeCun (2022) suggests that, despite data augmentation being such a prevalent method of improving model performance, it may actually prove a risk to blindly

turn to this technique regardless of dataset and approach. This appears to be a part of a larger phenomenon concerning a tendency of parametrized regularization measures to sacrifice performance on certain classes in favor of overall model accuracy. However, it is also caused in large part by the fact that different image transformations seem to possess varying levels of label preservation (Cui, Goel, and Kingsbury 2015; Taylor and Nitschke 2018) dependent on the class of image data, and, as such, can have a severe class-specific negative impact on the model performance by virtue of incurring label loss if applied too aggressively. This impact can also be so deep as to even impact downstream performance in the case of transfer learning tasks.

It may be a natural reaction, as such, to caution against using data augmentation as a regularization technique to avoid this. However, this can prove to be difficult in practice, as the overall performance boost this technique provides is undeniable, and it is currently used ubiquitously, with few alternatives. In addition, as alluded to before, the paper showed that other regularization methods, such as weight decay, can also be subject to this phenomenon. It is also important to note that Balestriero, Bottou, and LeCun (2022) claims that the phenomenon is model-agnostic for popular CNNs based on residual blocks such as ResNet (He et al. 2015), DenseNet (Huang, Liu, and Weinberger 2016), and others, but does not make any claims in regards to whether the phenomenon is data-agnostic, or how it would manifest in image classification networks that belong to architectures founded in considerably different principles, such as Vision Transformers (Dosovitskiy et al. 2020b; Liu et al. 2021) that use patch-based image processing and self-attention mechanisms to extract features from images.

Our work follows a course of further investigation. To formulate our primary research question, we follow the tenets of the data-centric AI movement championed by Andrew Ng, which seeks to systematically engineer the data used in training AI systems, and places special focus on accounting for imperfections in real world data. In data augmentation, the discipline outlines issues such as domain gaps, data bias and noise. Following this school of thought leads us to question if class-specific bias from data augmentations affect datasets different from Imagenet, in a different way. In particular, we seek to test whether this phenomenon can be observed on datasets that differ in nature to various degrees from Imagenet (Deng et al. 2009), which was used in Balestriero’s 2022 paper, and to what extent. To supplement this line of validation, another, secondary research question emerged from a seemingly minor detail in the original study. Concretely, we investigate if the addition of Random Horizontal Flipping have an effect on how the class-specific bias phenomenon manifests.

While not our core focus, we also seek to confirm how model-agnostic this phenomenon is on these new datasets. For this, it is first necessary to test with a model that has common features with ResNet50, which was the baseline for many experiments in (Balestriero, Bottou, and LeCun 2022). We selected EfficientNet, first described in Tan and Le (2019), which is a family of models that also utilizes residual blocks, but was designed via a neural architecture search (Elsken, Metzen, and Hutter 2019) using a new scaling method that uniformly scales all dimensions of model depth/width/resolution using a simple yet highly effective compound coefficient. To that end, we question if class-specific bias from data augmentations on the same dataset would affect a different Residual CNN architecture in the same manner as it would a ResNet. Finally, it is also worth investigating the effects of a vastly different architecture, as mentioned earlier. For these purposes, we have selected to use a SWIN Transformer, which is a relatively small patch-based vision transformer that uses a novel shifted windowing technique for more efficient computation of the self-attention mechanism that is inherent to Transformer-type models (Liu et al. 2021). Finally, we consider if class-specific bias from data augmentations on the same dataset would affect a Vision Transformer model in the same manner as it would a ResNet.

2 The Effect Of Data Augmentation-Induced Class-Specific Bias Is Influenced By Data, Regularization and Architecture

This section details our study’s data-centric and model-centric analysis of the phenomena originally observed in (Balestriero, Bottou, and LeCun 2022). Firstly, we establish a practical framework for replicating such experiments in Section 2.1. Following this, we use a ResNet50 model trained from scratch with the Random Cropping and Random Horizontal Flip DA to provide the data-centric analysis of DA-induced class-specific bias on three datasets (Fashion-MNIST, CIFAR-10 and CIFAR-100) in Section 2.2. We then take a step back in Section 2.3 to evaluate the potential side effects of including the Random Horizontal Flip augmentation, as

done in the original study. Finally, we conclude by demonstrating how alternate computer vision architectures interact with the phenomenon illustrated in previous sections. These findings are key as they serve to deepen our understanding of the potential pitfalls of introducing DA to computer vision tasks in order to improve overall model performance, while showing how the problem of class-specific bias can be alleviated or forestalled.

2.1 Data Augmentation Robustness Scouting

In this section, we seek to formalize a "bare minimum" procedure necessary to adopt and replicate an experiment framework for assessing the tradeoff between overall model performance, DA intensity and class-specific bias by outlining the specifics of our experiments' practical implementation. The goal of this is to serve as a guideline for applying the findings of [Balestriero, Bottou, and LeCun \(2022\)](#) in a more efficient manner that is better fit for practical or "business" environments, as well to lay the groundwork for procuring the results that shall be discussed in further sections of this chapter.

We propose the following procedure, further referred to as "Data Augmentation Robustness Scouting": First, a set of computer vision architectures is to be selected for a given dataset and DA regimen. Following this, the model is trained on a subset of the data in several training runs, such that each run features an increasing intensity of augmentation (represented by as a function of α). The test set performance (per-class and overall) is then measured for every value of α , such that dynamics in performance can be observed as α is gradually increased. This procedure is then repeated from start to end, with the performance being averaged out for every value of α to smooth out any fluctuations resulting from the stochastic nature of the training process. The granularity (expressed through the amount and range of α steps and amount of runs per value of α) should be kept to a bare necessary minimum such that the desired clarity required to observe trends in performance dynamics over different α values can be achieved. Following this study, if "ranges of interest" in α are established, it is recommended to perform the described procedure again with higher granularity within those ranges.

The experiments detailed in further sections of this chapter featured the DA Robustness Scouting procedure performed on three datasets - Fashion-MNIST, CIFAR-10 and CIFAR-100 ([Xiao, Rasul, and Vollgraf 2017](#); [Krizhevsky, Hinton et al. 2009](#)). The Random Cropping DA was evaluated, along with Random Horizontal Flip as a fixed supplementary augmentation. For our purposes, the preliminary model tuning and experiments were implemented using the Tensorflow and Keras libraries for Python. Our approach was based on best optimization practices for training convolutional neural networks as described in [Goodfellow, Bengio, and Courville \(2016d\)](#). Before an experiment can be run, a given model is repeatedly trained from scratch on a given dataset with a set of different permutations of learning rate, maximum epoch and batch size parameters. This was done in order to achieve a "best case" base model - one that did not use any overt regularization (so as not to obscure the impact of regularization during the experiment), provided the best possible performance on the test set, and was the least overfitted. As batch size tuning can be considered a form of regularization, only minimal tuning was applied to batch size to ensure sufficient model stability and performance. A validation subset (10% of the training set - common value used) was used to evaluate overfitting. It is important to note that the definition of "sufficient" is very dataset-specific, as some datasets lend themselves much more easily to being "solved" by models such as ResNet50 - both in terms of training error and generalization. Typically, regularization is used for the very purpose of helping improve generalization, but in the case of this study doing so would risk obscuring the phenomenon being observed. As such, a decision was made to "settle" that "best" base performance on some datasets would be considered subpar *ceteris paribus*.

The ResNet50 architecture was directly downloaded from Tensorflow's computer vision model zoo sans the Imagenet weights, as the models would be trained from scratch. [Balestriero, Bottou, and LeCun \(2022\)](#) makes no mention of the optimizer used, so the Adam optimizer ([Kingma and Ba 2014](#)) was used in all tuning and experiment steps. Each combination of model and dataset was tuned across a set of learning rates, epoch counts and batch sizes selected with the goal of getting the best validation and test set accuracies (using the `sparse_categorical_accuracy` metric from Keras) while being mindful of models' tendency towards overfitting.

The "small" EfficientNetV2S ([Tan and Le 2021](#)) architecture was selected for its respective experiment due to being a modern and time-efficient implementation of the EfficientNet family of models. The model was downloaded, tuned and optimized as per the above procedure.

The SWIN Transformer architecture was implemented based on existing Keras documentation, which was inspired by the original approach used in Liu et al. (2021), processing image data using 2x2 patches (about 1/16 of the image per patch, similar to Dosovitskiy et al. (2020a)) and using an attention window size of 2 and a shifting window size of 1. However, this approach originally included built-in regularization methods that deviated from our base experiment structure, such as random cropping and flipping already built into the model, label smoothing and an AdamW optimizer (Loshchilov and Hutter 2017), which features decoupled weight decay. These were all omitted from the base model used in tuning and further experiments, while maintaining the core architecture.

As it is generally widespread and commonly used as a data augmentation technique, the particular Random Crop procedure to be used was not well-defined in the text of Balestriero, Bottou, and LeCun (2022). As such, for the purposes of this study, the Random Crop data augmentation was defined as applying the “random crop” transformation from Tensorflow’s image processing library to the training dataset at every iteration, with the resulting image height and width calculated using the following formula:

$$new_image_size = round(image_size * (1 - \alpha))$$

Where α is a percentage or fraction representing the portion of the image that would be omitted and round() is the default Python. No padding was used. After being cropped, the images were upscaled back up to their original size so that they would still match the input layer requirements of 32x32px that the model trained on them required. In addition, these dimensions also mean that the test images do not need to be cropped down to the new size, which would be the more likely scenario in practice.

Finally, in order to accommodate existing limitations in available computing, the granularity of the experiments was reduced from 20 models per Random Crop transformation alpha to 4, as well as adjusting α in steps of 3-4%, rather than evaluating every 1%. To ensure the results maintained integrity, the exact figures for this granularity reduction were motivated by finding the minimum number of runs which corresponded to insignificant marginal deviations in the resulting mean test accuracy per additional run, preserving the expected trend. The new granularity of the augmentation alpha was determined based on the observation that the original paper’s highlighted trends in accuracy would still persist if this smoothing was applied to them, if not become simpler to detect by virtue of eliminating the existing fluctuations. In addition, using steps of Random Crop α that were finer would produce the same dimensions in post-crop training images due to the rounding involved and the images’ small size, leading to multiple iterations which would be practically identical, thus creating redundancy.

Additionally, in the case of all conducted experiments, the Keras callback implementation of Early Stopping was used with a 10% validation subset separated from the main training subset. It is a popular deep learning technique that monitors some metric after each training epoch (typically, loss or a select accuracy metric on the validation subset) and terminates training if it fails to perform better than a previous evaluation in a number of epochs described by the “patience” parameter. This algorithm also commonly features an optional restoration of model weights to the best-performing epoch. Early Stopping is commonly recognized as a regularization technique - however, it is considered unobtrusive, as it requires almost no change in the underlying training procedure, and can also be thought of as a “very efficient hyperparameter selection algorithm” (Goodfellow, Bengio, and Courville 2016d). As this work concerns the effects of regularization, a decision was made that Early Stopping must be used cautiously, to minimum effect, despite its unobtrusive nature.

2.2 The Specifics Of Data Affect Augmentation-Induced Bias

As a key part of our data-centric analysis of the bias-inducing effects of DA detailed by Balestriero, Bottou, and LeCun (2022), we conducted a series of experiments based on the paper’s initial proposal of training and evaluating a set of CNN models while adjusting a DA regime represented as a function of some parameter α between batches of runs (see Figure 2 for results). To focus the scope of our research, we have limited the experiments in this section to using ResNet50 as the architecture of choice, with Random Horizontal Flipping applied combined with Random Cropping with increasing portions of the training images obscured as the parametrized augmentation. For illustrative purposes, three datasets were chosen for the purposes of the trial to provide a relative diversity of content: Fashion-MNIST, CIFAR-10 and CIFAR-100. All three datasets differ from ImageNet in possessing a much smaller image quantity (< 100K vs. > 1M), class

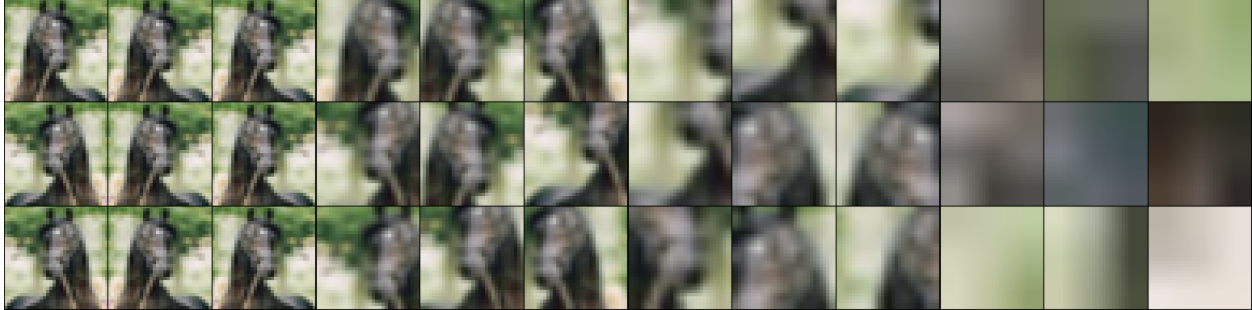


Figure 1: This figure shows a collection of four 3x3 grids, each demonstrating the effect of a Random Crop + Random Horizontal Flip combined data augmentation on an image belonging to the "horse" class of the CIFAR-10 dataset. The Random Crop α for is 0%, 30%, 60% and 90% for each grid, respectively. Label loss progression can be intuited to a degree, as the proportion of images that lack the distinctive features of the "horse" class increases with α .

count (≤ 100 vs. $> 1K$), and image size ($< 40px$ vs. $> 200px$). There are some additional distinctions: Fashion-MNIST consists of greyscale top-down photos of clothing items, whereas CIFAR-100 has very few images per class, despite CIFAR datasets being otherwise quite close in subject matter to ImageNet.

Despite significantly fewer runs, the results of our experiments do clearly illustrate the label-erasing effect of excessive DA application and its strong variation between classes, as seen, for example, in the performances of the Coat, Dress, Shirt and Sandal in Figure 2, each of which experiences distinctive performance dynamics as α increases, and each category has a different threshold of α past which label-loss from Random Cropping occurs rapidly (as illustrated by a rapid drop-off in test set accuracy). In addition to confirming class-specific DA-induced bias, we observe a very clear difference across the three datasets in terms of the speed at which this effect is seen in mean performance, as well as the degree of difference between individual classes. This can be attributed to the complexity of each dataset, but also clearly illustrates how "robustness" to class-specific bias from DA can vary heavily between datasets in the same way as it can between classes. While this difference is noticeable between the three observed datasets, it is even more stark when compared to ImageNet's performance in Balestrieri, Bottou, and LeCun (2022), as label loss and corresponding mean test set performance decline occur at much earlier values of α in our observations.

As in Balestrieri, Bottou, and LeCun (2022), mean test set performance in all cases follows a trend of "increase, fall, level off" as α pushes all but the most robust classes past the threshold of complete label loss (for example, in the Figure 2, the mean accuracy on CIFAR-10 reaches its highest point of 0.764 at 10% α , then rapidly declines until an α of 70%, after which it levels off at around 0.21. On the other hand, the Fashion-MNIST plot is very illustrative of class-specific behaviors, as we see the "Sandal" class reach its peak accuracy of 0.994 at an α as late as 36%, while "Coat" begins to drop from 0.86 down to near-zero accuracies as early as 10% and 43%, respectively. For a full summary of the diverse α at which each class and mean test set performance reach their peak, see Appendices F, G and H.

The causes of this dataset-specific bias robustness can be narrowed to two causes - overall complexity as a learning task (e.g. Fashion-MNIST is "simple to solve", and thus experiences minimal benefit from regularization before reaching detriment), as well as robustness to label loss from a given DA, which can occur on dataset or class level. Class-level robustness can be illustrated by comparing the performance of the T-Shirt and Trouser classes in Figure 2, as images belonging to the Trouser class are quite visually distinct from most other categories even at higher levels of cropping, while the T-Shirt class quickly loses its identity with increased α values, manifesting in the visible performance difference. Dataset-level robustness can occur due to such factors as training images containing more information (e.g. "zoomed-out" depictions of objects, higher image size, as well as RGB color), and can be seen in how the CIFAR datasets' mean performance and its dynamics relative to α compare to Fashion-MNIST.

Here, a promising direction for research could be to conduct a range of similar experiments on datasets picked out specifically with this robustness to a particular DA in mind - for example, a dataset such as the Describable Textures Dataset (Cimpoi et al. 2014) consists of images of objects with a focus on texture, with 47 classes, such as "braided", "dotted", "honeycombed", "woven". By nature, textures are repeating

patterns, and as such, at least some of the featured classes should be very resilient to random cropping. For example, if the image features a "chequered" texture with a 10x10 grid of squares, then cropping out up to 89% of the original image would still not obscure the pattern.

It is also worth noting that the mean performance decline in our experiments occurs at a more drastic rate than in [Balestriero, Bottou, and LeCun \(2022\)](#). This could have been caused by differences in DA implementation, but could also stem from differences in the training data used. For example, while a human observer may conclude that the same amount of information is being removed by cropping images using the same α , this is not the case from a model's perspective, as the absolute count of pixels removed by this operation depends on the original size of the images. This, in turn, is another possible avenue for future inquiry: experiments could be run on entirely new datasets with varying image sizes, or alternatively, on the same datasets used in this work, but with the training images upscaled.

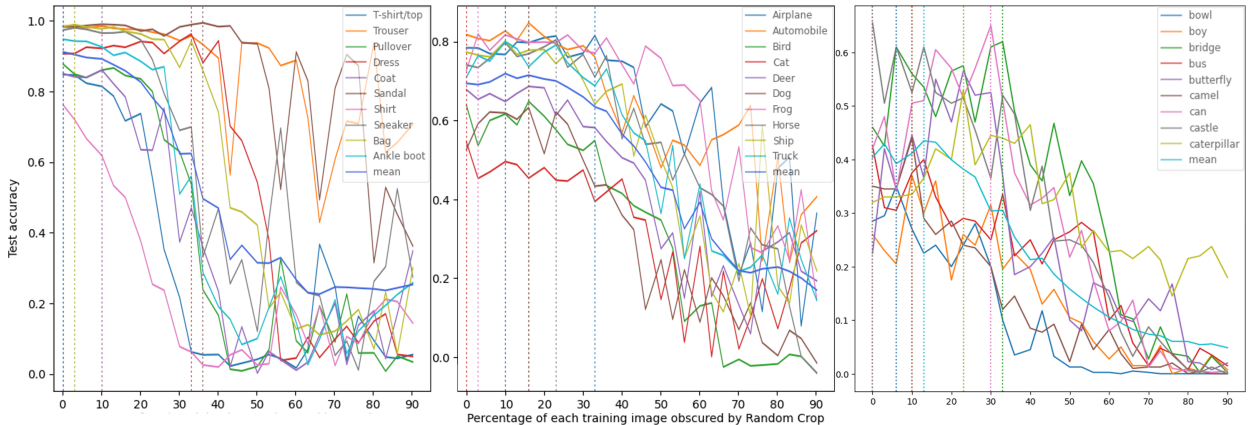


Figure 2: The results in this figure employ official ResNet50 models from Tensorflow trained from scratch on the Fashion-MNIST, CIFAR-10 & CIFAR-100 datasets respectively, with the Random Crop and Random Horizontal Flip DA applied. All results in this figure are averaged over 4 runs. During training, the proportion of the original image obscured by the augmentation varies from 100% to 10%. We observe that, in line with expectations, training the same architecture on with varying random crop percentage can provide greater average test accuracy (blue) up to a certain point, but does eventually drop due to the acute negative impact some per-class accuracies experience past given crop α values. The vertical dotted lines denote the best test accuracy for every class. Only a subset of classes is shown for CIFAR-100 for legibility purposes.

2.3 Adding Random Horizontal Flipping Contributes To Augmentation-Induced Bias

As part of this work's goal was to confirm the effects of DA on the bias-variance trade-off of image classification problems as seen in [Balestriero, Bottou, and LeCun \(2022\)](#), we also chose to delve deeper into the specifics of the DA policy implemented by the original paper. In particular, we felt that it overlooked the possible effects its universal application of Random Horizontal Flipping (henceforth "RHF") as a supplemental DA may have introduced. In an effort to investigate this, we once again conducted a series of experiments similar to Section 2.2, this time excluding RHF.

Our trials showed (see Figure 3 and appendices F, J and K) similar trends and results when compared to Section 2.1. However, as could be expected from removing a minor source of regularization such as RHF, overall mean performance was marginally worse across all three datasets. In addition, it appears that the thresholds of α (past which overall and class-specific performances begin to fall, as well as at which best per-class and mean accuracies are reached) have generally increased - for example, "Sandal"'s best performance is up to 40% from 36% compared to the previous section. In this way, we see that RHF compounds with the scaling Random Cropping DA, acting as a "constant" source of additional regularization, while preserving, if accelerating, the dynamics of test set accuracies as α grows. With this in mind, [Balestriero, Bottou, and LeCun \(2022\)](#) is validated, as the conclusions reached in the work would likely not have been impacted had

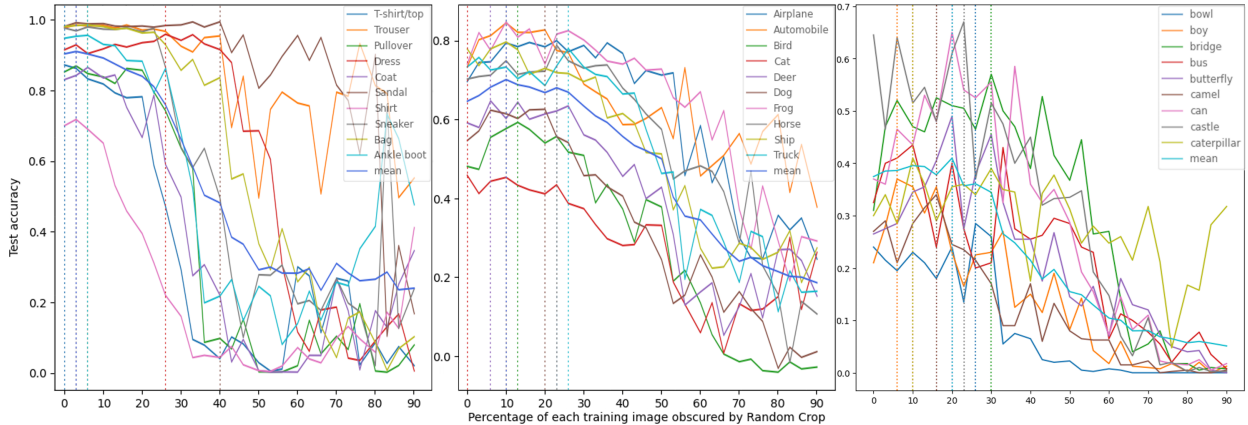


Figure 3: The results in this figure employ official ResNet50 models from Tensorflow trained from scratch on the Fashion-MNIST, CIFAR-10 & CIFAR-100 datasets respectively, with the Random Crop but no Random Horizontal Flip DA applied. All results in this figure are averaged over 4 runs. During training, the proportion of the original image obscured by the augmentation varies from 100% to 10%. We observe that while the trends from Figure 2 are generally maintained, the removal of Random Flip seems to decrease the speed at which class-specific bias manifests as α is increased. Only a subset of classes is shown for CIFAR-100 for legibility purposes.

RHF been omitted. While not gravely consequential, this finding should serve as a reminder that caution should be exercised when chaining a plurality of data augmentations together. While such an approach is standard practice in contemporary computer vision tasks, it can rapidly increase complexity, and controlling for the influence of a given augmentation on class-specific bias may become difficult.

2.4 Alternative Architectures Have Variable Effect On Augmentation-Induced Bias

Having carried out a data-centric analysis of DA-induced class-specific bias, we dedicated the last series of experiments (see Figure 4) to a more model-centric approach to the phenomenon. [Balestriero, Bottou, and LeCun \(2022\)](#) illustrates that different architectures tend to agree on the label-preserving regimes for DA(α) - in other words, that swapping ResNet50 for a different model in the above experiments would not yield a notable difference in resulting class-specific and overall performance dynamics. To validate and expand on this claim, we recreated the experiment from Section 2.2 on the Fashion-MNIST dataset using another residual CNN, EfficientNetV2S, as well as a Vision Transformer in SWIN-Transformer.

The "small" EfficientNetV2S ([Tan and Le 2021](#)) architecture was selected due to being a modern and time-efficient implementation of the EfficientNet family of models. The model was downloaded, tuned and optimized using a procedure matching previous sections. The EfficientNetV2S runs of this section's experiments seemed to further validate the original assumption that the phenomenon appears to be model-agnostic (though data-specific), at least for the residual family of CNNs, as the different complexity and size of the architecture did have an effect on the speed of class-specific bias occurring as the random crop α was increased, but the general dynamics of how performance evolved were preserved. For example, as can be seen in Figures 4, deterioration in per-class accuracy begins to occur rapidly for "Dress" at an α value of 30% for EfficientNetV2S, in contrast to 40% for ResNet50. For a full summary of the diverse α at which each class and mean test set performance reach their peak, see Appendix I.

With the previous section confirming the model-agnostic nature of the phenomenon as it pertains to residual CNNs, the final trial followed up by evaluating the performance of a SWIN Transformer, as the architecture is composed in a fundamentally different way, and can be adjusted to perceive images with a finer level of granularity via the patch size parameter. The model was prepared similarly to previous sections. As visible in Figure 4 and Appendix L, while the use of a Vision Transformer model did not entirely avert the overall class-specific bias trend as random cropping was applied more aggressively, it severely delayed

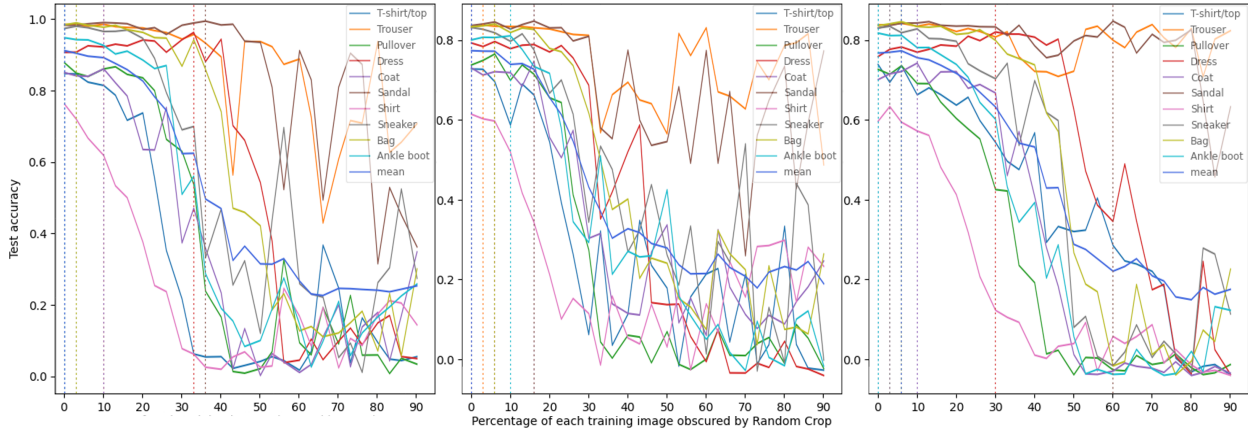


Figure 4: The results in this figure employ official ResNet50, EfficientNetV2S and SWIN-Transformer models from Tensorflow trained from scratch on the Fashion-MNIST dataset, with the random crop and random horizontal flip DA applied. All results in this figure are averaged over 4 runs. During training, the proportion of the original image obscured by the augmentation varies from 100% to 10%. We observe that ResNet50 and EfficientNetV2S display very similar trends, whereas SWIN Transformer displays a noticeably delayed decline in onset of class-specific bias for certain classes.

its heavier impacts, and even noticeably changed the behavior of certain classes (for example, maintaining the stability of the top performers in "Trouser" and "Sandal" even for very high values of α , while delaying "Dress" and "Coat"'s rapid deterioration in accuracy to 47% and 30% from 40% and 23%, respectively) in effect making the model-dataset combination more robust against the potential negative trade-offs data augmentation can bring. Despite this, and being similar in terms of computational requirements, its best performance achieved in practice was marginally lower than that of ResNet50. While it does not outright disagree with [Balestriero, Bottou, and LeCun \(2022\)](#)'s model-agnostic proposition, the implications of this result are such that architectures for computer vision tasks can and should be chosen not just by best overall test set performance, but also based on other merits, such as robustness to bias and label loss resulting from aggressive data augmentations, especially in cases where such augmentations are expected to be applied en masse or without intensive monitoring, such as in MLOps systems with regular retraining.

While the above experiment does serve to illustrate the potential merit of applying alternative architectures in the context of regulating DA-induced class-specific bias, broader research is likely warranted. A natural direction of such an extension may be to continue with applying different families and instances of image-classifying neural network architectures to the task. One option is to expand the research utilizing SWIN Transformer by testing it on a further plurality of datasets with a wider variety of patch sizes, as the concepts of regulating the granularity with which the model learns to see details in images and the random cropping DA are conceptually adjacent. Following this, exploring the same problem with different Vision Transformers, such as the more lightweight MobileViT ([Mehta and Rastegari 2021](#)) or Google's family of large ViT models ([Zhai et al. 2022](#)) is another step in that direction. Another possible direction to explore the model-specific degree of the phenomenon is to investigate how it pertains to Capsule Networks, first described in [Sabour, Frosst, and Hinton \(2017\)](#), as the architecture, once again, vastly differs from both Residual CNNs and Vision Transformers, and is generally considered to be less susceptible to variance from image transformations. This family of models is also very demanding to train, and would require a greater investment of resources or smaller scope than what our work had. As CapsNets are, at the time of writing, a very active area of research ([Kwabena Patrick et al. 2022](#)), we recommend this as a very valuable line of inquiry.

3 Conclusion and Limitations

This study extends the analysis initiated by [Balestriero, Bottou, and LeCun \(2022\)](#), focusing on the impact of data augmentations, particularly Random Crop, on class-specific bias in image classification models. Our contributions are multi-faceted, addressing the need for a more nuanced understanding of DA’s effects across different contexts.

We empirically demonstrate that DA-induced class-specific biases are not exclusive to ImageNet but also affect datasets with distinct characteristics, such as Fashion-MNIST and CIFAR. These datasets, featuring significantly fewer and smaller-sized images, some of which are monochrome, provide a broader canvas to assess DA’s impact. This variation in dataset characteristics allowed us to explore how DA-induced biases manifest in environments markedly different from ImageNet, thus broadening the scope of understanding regarding DA’s implications.

By incorporating additional deep neural network architectures like EfficientNetV2S (a residual model) and SWIN Vision Transformer (a non-residual, patch-based model), we delve into the model-agnostic proposition of class-specific DA-induced bias. Our findings reveal that while the phenomenon extends to residual models, alternative architectures such as Vision Transformers exhibit a varying degree of robustness or altered dynamics in response to DA, suggesting a potential strategy for mitigating class-specific biases through architectural selection.

We offer a detailed methodology for "data augmentation robustness scouting," refining the initial concept proposed by [Balestriero, Bottou, and LeCun \(2022\)](#). This step-by-step approach aims at a more efficient, resource-sensitive examination of DA’s effects, facilitating the identification and mitigation of class-specific biases in the model design phase. By applying this methodology, we not only validate previous findings but also present a practical framework for future studies and model development efforts.

Our study, while highlighting the aforementioned contributions, acknowledges its scope limitations concerning the variety of architectures and datasets examined. Future work is encouraged to explore a broader array of computer vision models and data characteristics, potentially unveiling novel insights into DA’s nuanced effects on model performance and bias. This endeavor aims not only to deepen our understanding of DA’s impact across different settings but also to contribute to the development of more equitable and effective computer vision systems.

References

- Balestriero, Randall, Leon Bottou, and Yann LeCun. 2022. The effects of regularization and data augmentation are class dependent. In *Advances in Neural Information Processing Systems*, volume 35, pages 37878–37891, Curran Associates, Inc.
- Bishop, Christopher M and Nasser M Nasrabadi. 2006. *Pattern recognition and machine learning*, volume 4. Springer.
- Cimpoi, M., S. Maji, I. Kokkinos, S. Mohamed, , and A. Vedaldi. 2014. Describing textures in the wild. In *Proceedings of the IEEE Conf. on Computer Vision and Pattern Recognition (CVPR)*.
- Cui, Xiaodong, Vaibhava Goel, and Brian Kingsbury. 2015. Data augmentation for deep neural network acoustic modeling. *IEEE/ACM Trans. Audio, Speech and Lang. Proc.*, 23(9):1469–1477.
- Deng, Jia, Wei Dong, Richard Socher, Li-Jia Li, Kai Li, and Li Fei-Fei. 2009. Imagenet: A large-scale hierarchical image database. In *2009 IEEE conference on computer vision and pattern recognition*, pages 248–255, Ieee.
- Dosovitskiy, Alexey, Lucas Beyer, Alexander Kolesnikov, Dirk Weissenborn, Xiaohua Zhai, Thomas Unterthiner, Mostafa Dehghani, Matthias Minderer, Georg Heigold, Sylvain Gelly, Jakob Uszkoreit, and Neil Houlsby. 2020a. An image is worth 16x16 words: Transformers for image recognition at scale. *CoRR*, abs/2010.11929.
- Dosovitskiy, Alexey, Lucas Beyer, Alexander Kolesnikov, Dirk Weissenborn, Xiaohua Zhai, Thomas Unterthiner, Mostafa Dehghani, Matthias Minderer, Georg Heigold, Sylvain Gelly, et al. 2020b. An image is worth 16x16 words: Transformers for image recognition at scale. *arXiv preprint arXiv:2010.11929*.
- Elsken, Thomas, Jan Hendrik Metzen, and Frank Hutter. 2019. Neural architecture search: A survey. *The Journal of Machine Learning Research*, 20(1):1997–2017.
- Feng, Xin, Youni Jiang, Xuejiao Yang, Ming Du, and Xin Li. 2019. Computer vision algorithms and hardware implementations: A survey. *Integration*, 69:309–320.
- Goodfellow, Ian, Yoshua Bengio, and Aaron Courville. 2016a. *Deep Learning*, chapter 5. MIT Press. <http://www.deeplearningbook.org>.
- Goodfellow, Ian, Yoshua Bengio, and Aaron Courville. 2016b. *Deep Learning*, chapter 9. MIT Press. <http://www.deeplearningbook.org>.
- Goodfellow, Ian, Yoshua Bengio, and Aaron Courville. 2016c. *Deep Learning*, chapter 6. MIT Press. <http://www.deeplearningbook.org>.
- Goodfellow, Ian, Yoshua Bengio, and Aaron Courville. 2016d. *Deep Learning*, chapter 7. MIT Press. <http://www.deeplearningbook.org>.
- He, Kaiming, Xiangyu Zhang, Shaoqing Ren, and Jian Sun. 2015. Deep residual learning. *Image Recognition*, 7.
- Huang, Gao, Zhuang Liu, and Kilian Q. Weinberger. 2016. Densely connected convolutional networks. *CoRR*, abs/1608.06993.
- Kingma, Diederik P and Jimmy Ba. 2014. Adam: A method for stochastic optimization. *arXiv preprint arXiv:1412.6980*.
- Ko, Tom, Vijayaditya Peddinti, Daniel Povey, and Sanjeev Khudanpur. 2015. Audio augmentation for speech recognition. In *Sixteenth annual conference of the international speech communication association*.
- Krizhevsky, Alex, Geoffrey Hinton, et al. 2009. Learning multiple layers of features from tiny images.
- Kwabena Patrick, Mensah, Adebayo Felix Adekoya, Ayidzoe Abra Mighty, and Baagyire Y. Edward. 2022. Capsule networks – a survey. *Journal of King Saud University - Computer and Information Sciences*, 34(1):1295–1310.
- LeCun, Yann, Yoshua Bengio, et al. 1995. Convolutional networks for images, speech, and time series. *The handbook of brain theory and neural networks*, 3361(10):1995.
- LeCun, Yann, Léon Bottou, Yoshua Bengio, and Patrick Haffner. 1998. Gradient-based learning applied to document recognition. *Proceedings of the IEEE*, 86(11):2278–2324.

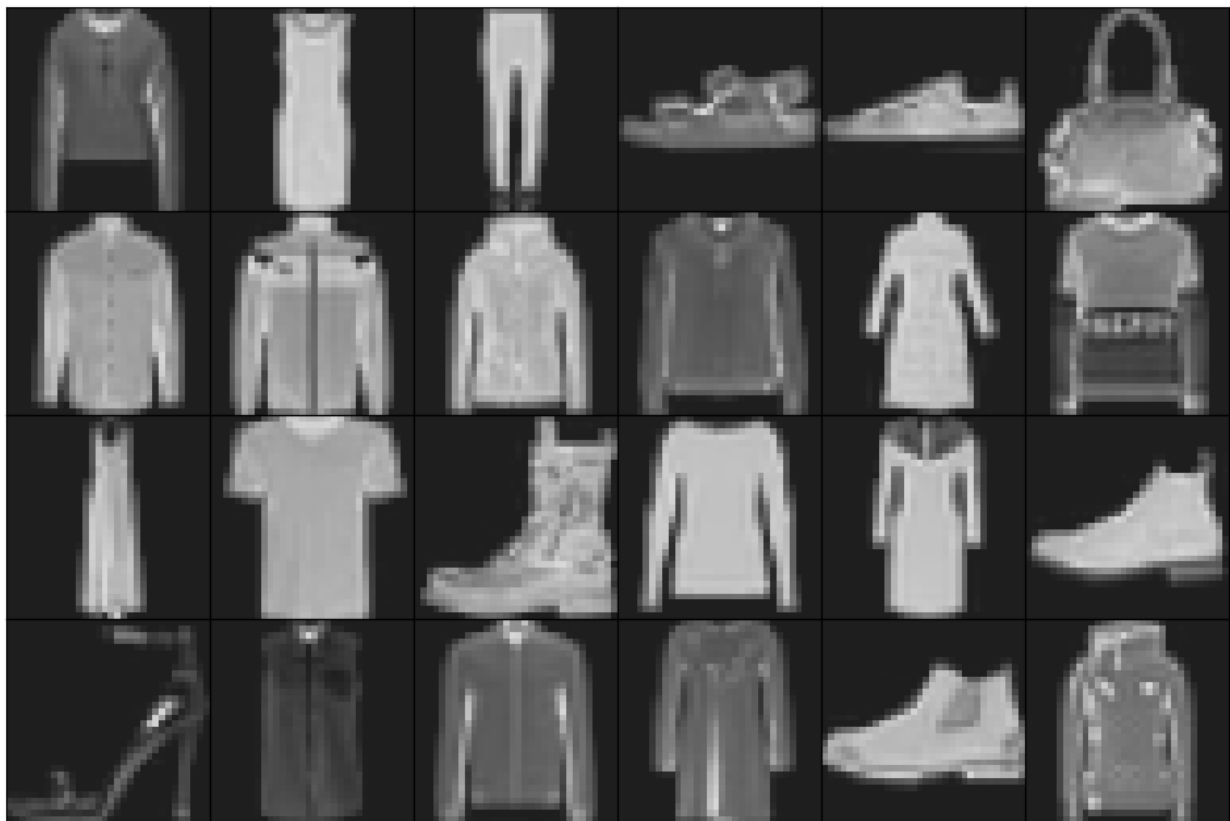
- LeCun, Yann, Koray Kavukcuoglu, and Clément F. Farabet. 2010. Convolutional networks and applications in vision. In *Proceedings of 2010 IEEE international symposium on circuits and systems*, pages 253–256, IEEE.
- Liu, Ze, Yutong Lin, Yue Cao, Han Hu, Yixuan Wei, Zheng Zhang, Stephen Lin, and Baining Guo. 2021. Swin transformer: Hierarchical vision transformer using shifted windows. In *Proceedings of the IEEE/CVF International Conference on Computer Vision (ICCV)*, pages 10012–10022.
- Loshchilov, Ilya and Frank Hutter. 2017. Decoupled weight decay regularization. *arXiv preprint arXiv:1711.05101*.
- Mehta, Sachin and Mohammad Rastegari. 2021. Mobilevit: Light-weight, general-purpose, and mobile-friendly vision transformer. *CoRR*, abs/2110.02178.
- Sabour, Sara, Nicholas Frosst, and Geoffrey E Hinton. 2017. Dynamic routing between capsules. *Advances in neural information processing systems*, 30.
- Shalev-Shwartz, Shai and Shai Ben-David. 2014. *Understanding machine learning: From theory to algorithms*. Cambridge university press.
- Shorten, Connor and Taghi M Khoshgoftaar. 2019. A survey on image data augmentation for deep learning. *Journal of big data*, 6(1):1–48.
- Tan, Mingxing and Quoc Le. 2019. EfficientNet: Rethinking model scaling for convolutional neural networks. In *Proceedings of the 36th International Conference on Machine Learning*, volume 97 of *Proceedings of Machine Learning Research*, pages 6105–6114, PMLR.
- Tan, Mingxing and Quoc V. Le. 2021. Efficientnetv2: Smaller models and faster training. *CoRR*, abs/2104.00298.
- Taylor, Luke and Geoff Nitschke. 2018. Improving deep learning with generic data augmentation. In *2018 IEEE symposium series on computational intelligence (SSCI)*, pages 1542–1547, IEEE.
- Tihonov, Andrei Nikolajevits. 1963. Solution of incorrectly formulated problems and the regularization method. *Soviet Math.*, 4:1035–1038.
- Tikhonov, Andrey Nikolayevich. 1943. On the stability of inverse problems. In *Dokl. Akad. Nauk SSSR*, volume 39, pages 195–198.
- Voulodimos, Athanasios, Nikolaos Doulamis, Anastasios Doulamis, Eftychios Protopapadakis, et al. 2018. Deep learning for computer vision: A brief review. *Computational intelligence and neuroscience*, 2018.
- Xiao, Han, Kashif Rasul, and Roland Vollgraf. 2017. Fashion-mnist: a novel image dataset for benchmarking machine learning algorithms. *arXiv preprint arXiv:1708.07747*.
- Zhai, Xiaohua, Alexander Kolesnikov, Neil Houlsby, and Lucas Beyer. 2022. Scaling vision transformers. In *Proceedings of the IEEE/CVF Conference on Computer Vision and Pattern Recognition (CVPR)*, pages 12104–12113.

Appendices

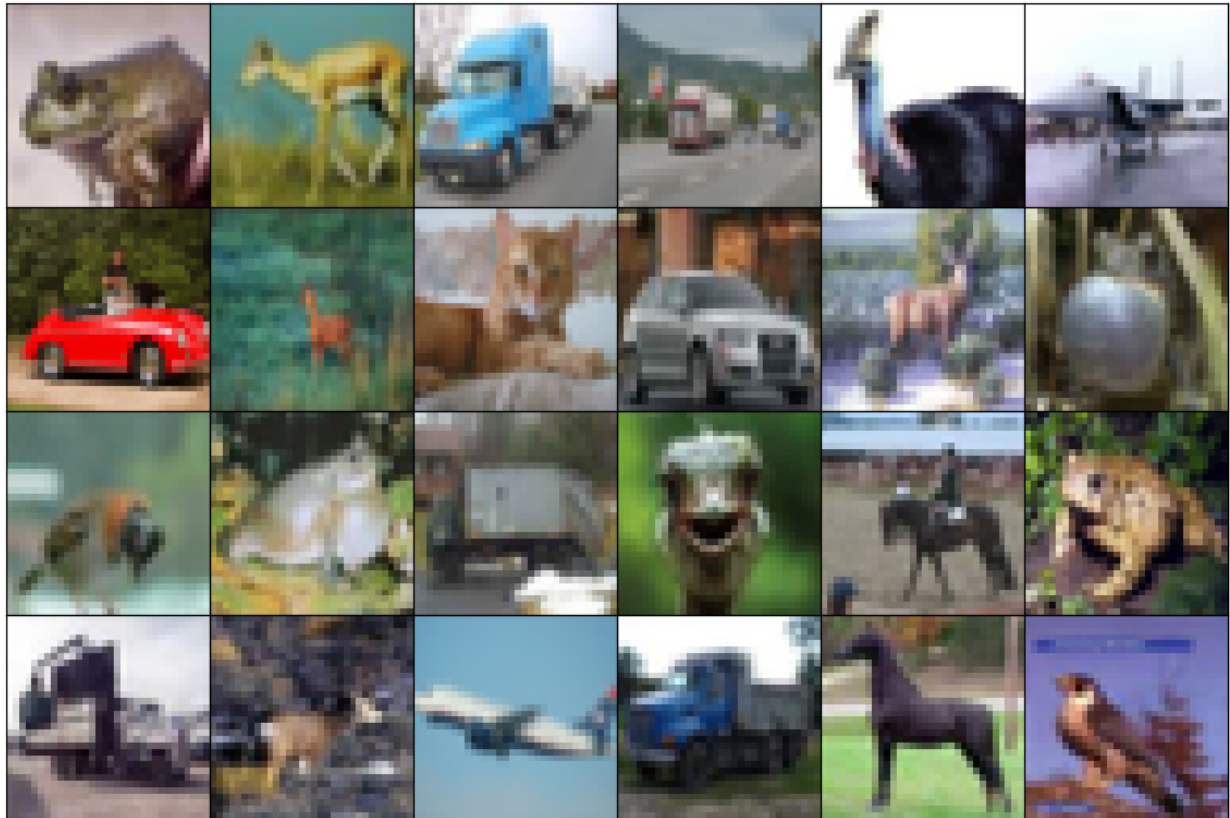
Appendix A: Image dimensions (in pixels) of training images after being randomly cropped and before being resized

[32x32, 31x31, 30x30,
29x29, 28x28, 27x27,
26x26, 25x25, 24x24,
22x22, 21x21, 20x20,
19x19, 18x18, 17x17,
16x16, 15x15, 14x14,
13x13, 12x12, 11x11,
10x10, 9x9, 8x8,
6x6, 5x5, 4x4, 3x3]

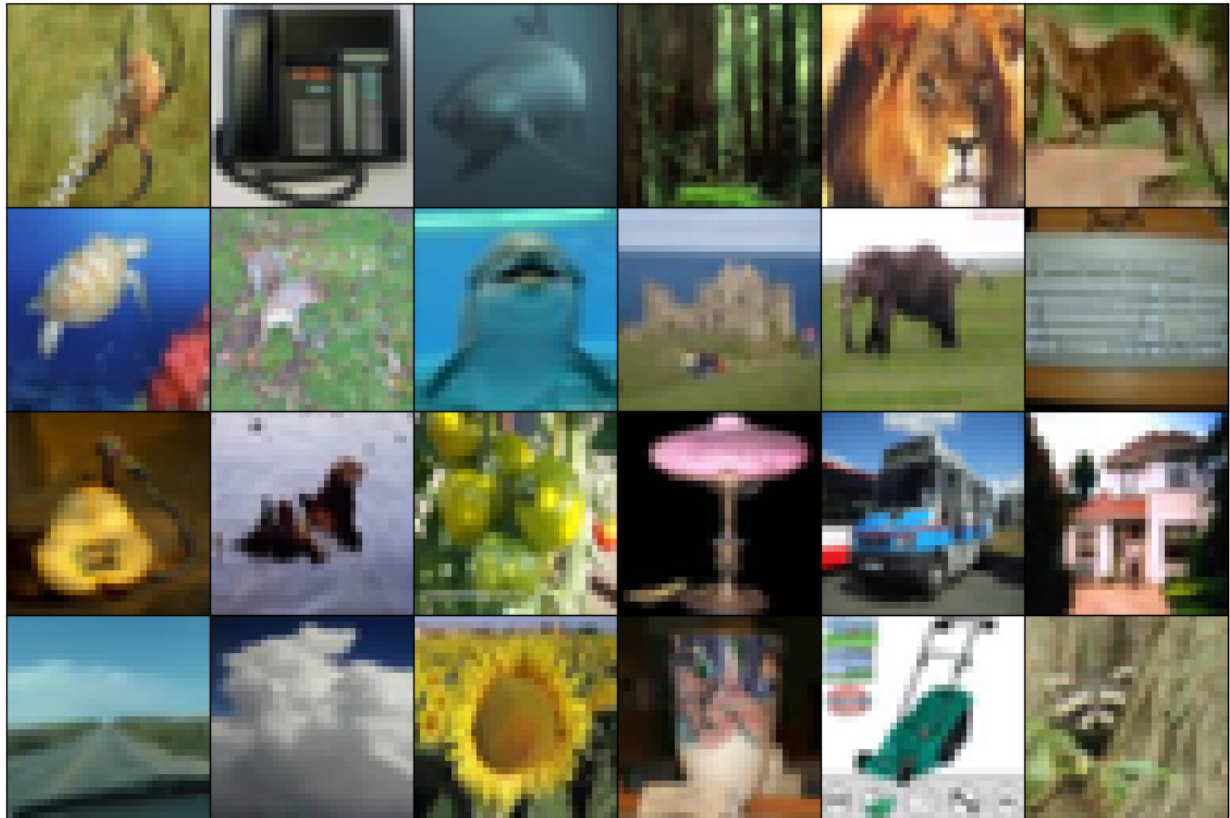
Appendix B: Dataset samples corresponding to the Fashion-MNIST segment used in training



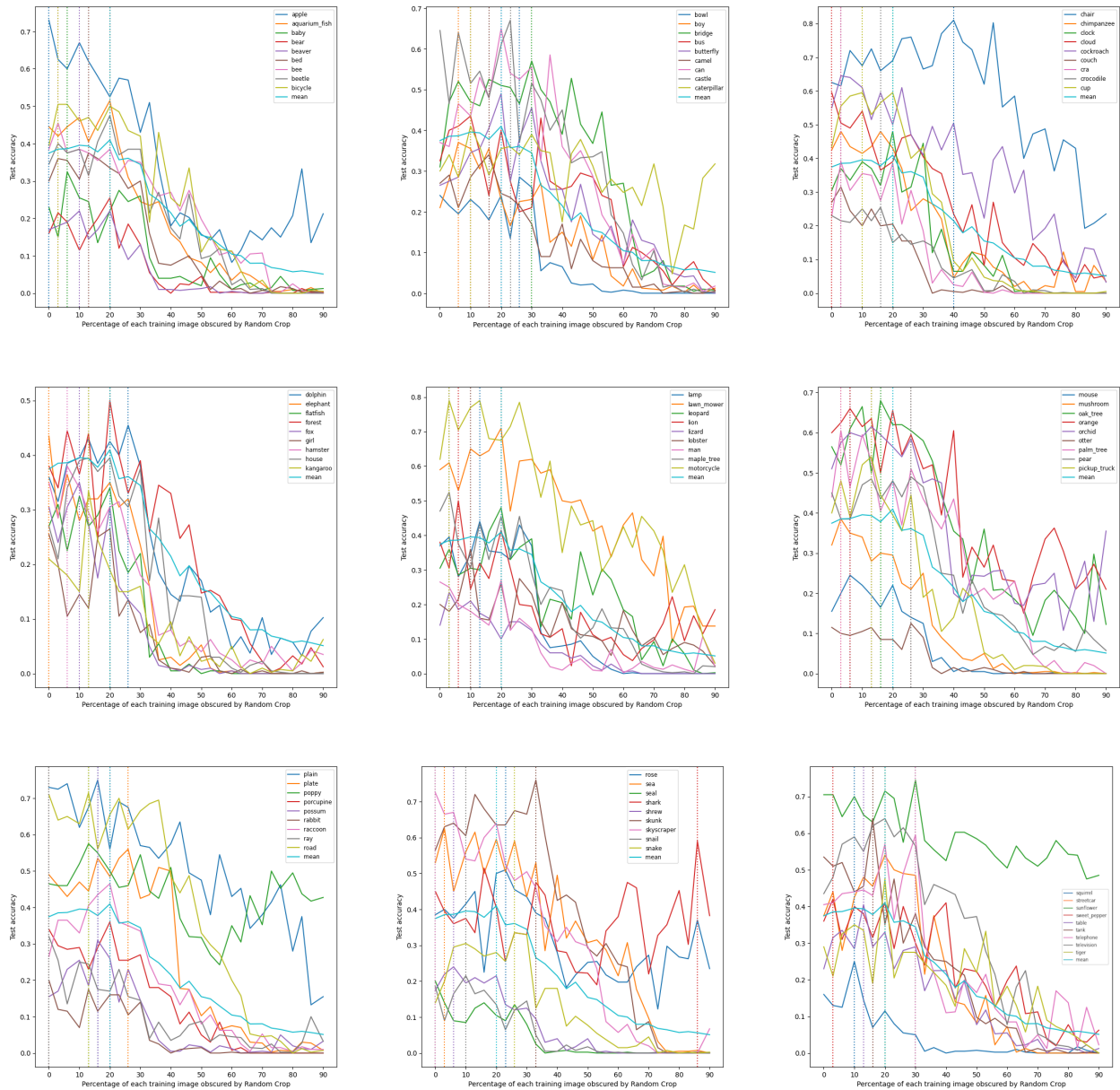
Appendix C: Dataset samples corresponding to the CIFAR-10 segment used in training

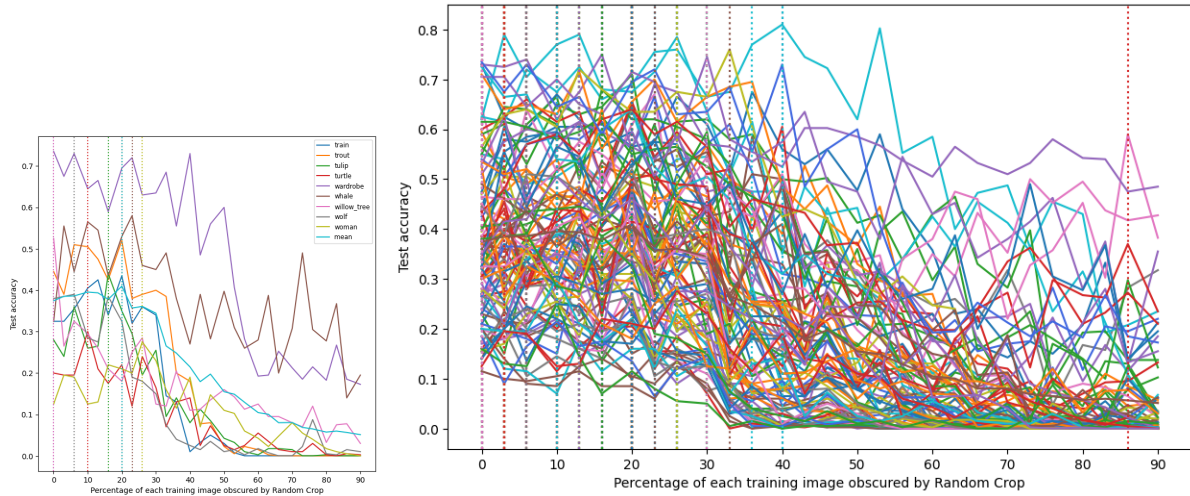


Appendix D: Dataset samples corresponding to the CIFAR-100 segment used in training

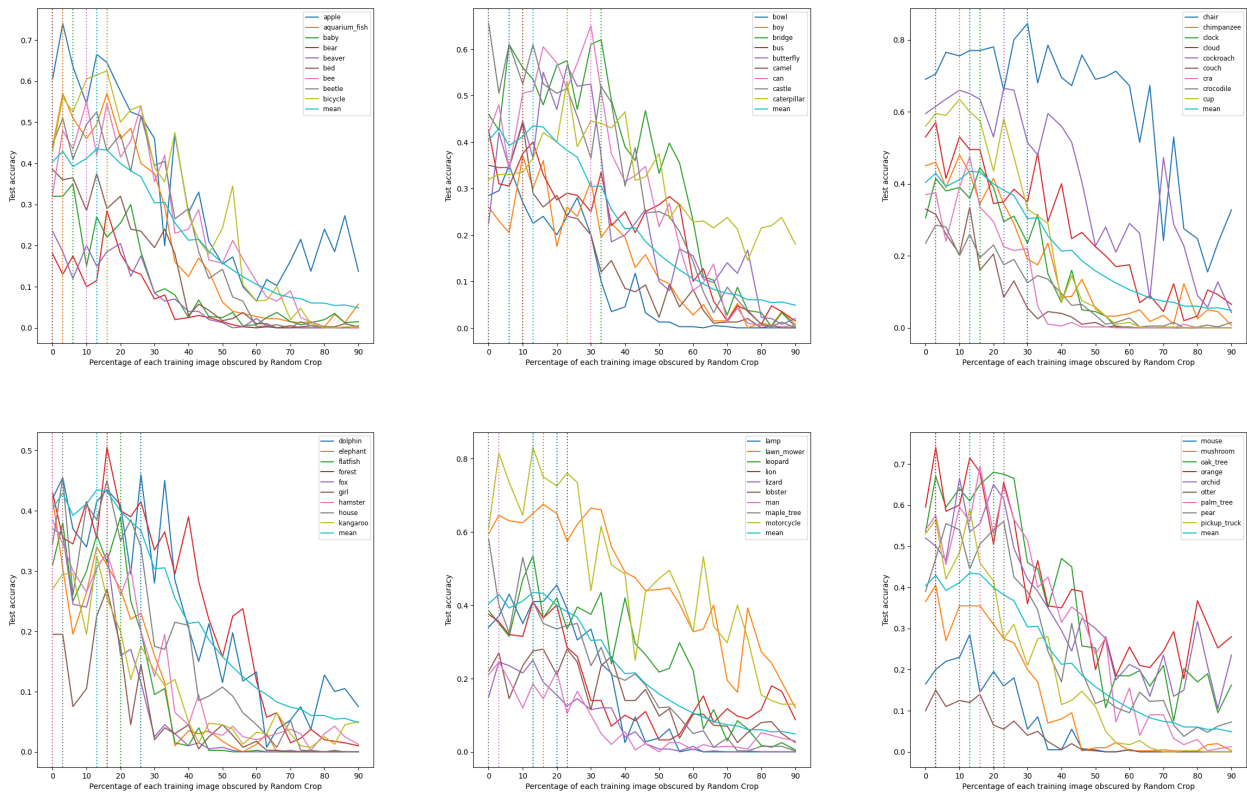


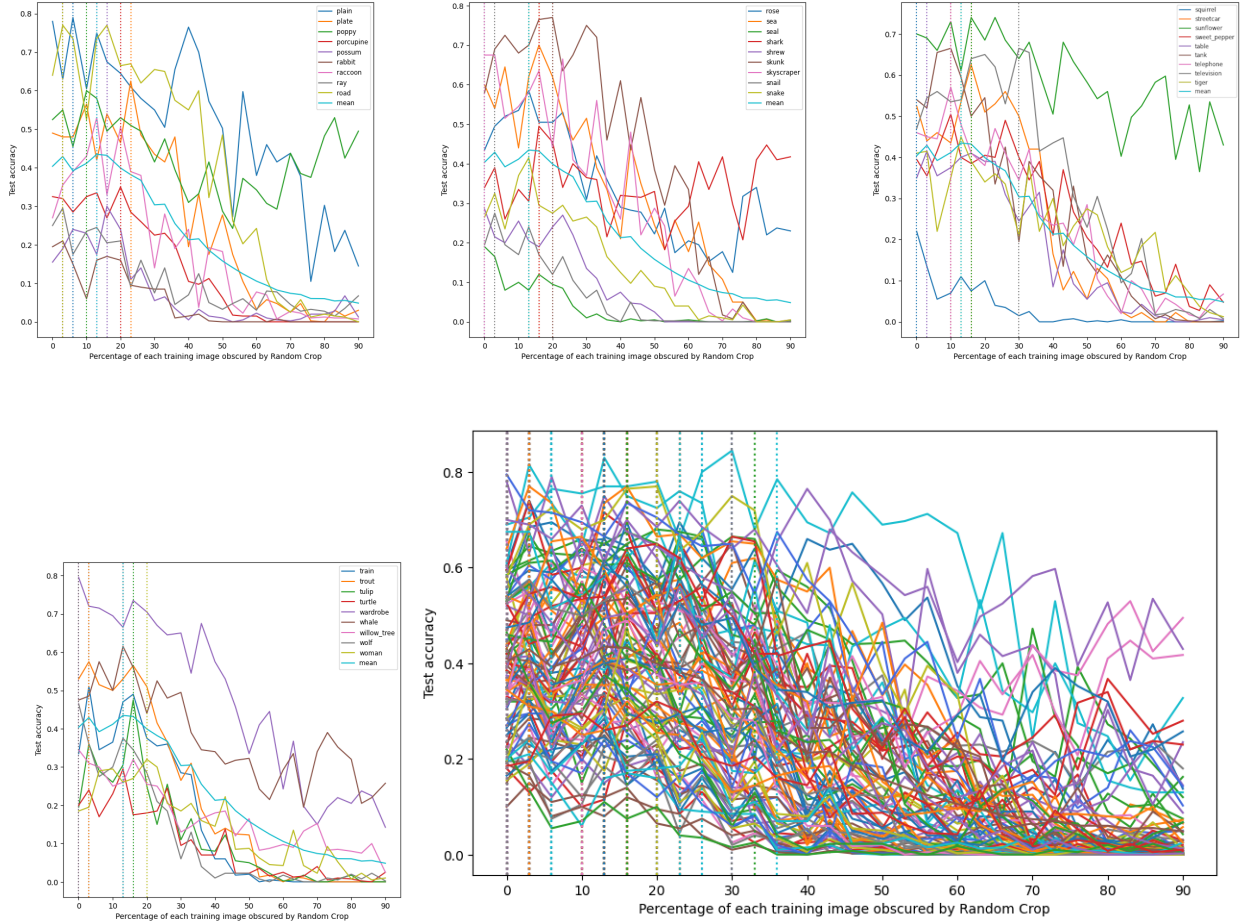
Appendix E: Full collection of class accuracy plots for CIFAR-100





(a) The results in all figures employ official ResNet50 models from Tensorflow trained from scratch on the CIFAR-100 dataset with random crop data augmentation applied. All results in this figure are averaged over 4 runs. During training, the proportion of the original image obscured by the augmentation varies from 100% to 10%. We observe The vertical dotted lines denote the best test accuracy for every class.





(a) The results in all figures employ official ResNet50 models from Tensorflow trained from scratch on the CIFAR-100 dataset with random crop and random horizontal flip data augmentations applied. All results in this figure are averaged over 4 runs. During training, the proportion of the original image obscured by the augmentation varies from 100% to 10%. We observe The vertical dotted lines denote the best test accuracy for every class.

Appendix F: Full collection of best test performances for CIFAR-100

Without Random Horizontal Flip:

	chair	motorcycle	skunk	plain	sunflower	wardrobe
Random Crop α	40	3	33	16	30	0
Test Accuracy	0.81	0.79	0.76	0.75	0.745	0.735
	apple	skyscraper	road	lawn_mower	oak_tree	keyboard
Random Crop α	0	0	13	20	16	36
Test Accuracy	0.73	0.725	0.715	0.71	0.68	0.675
	castle	mountain	orange	can	cockroach	television
Random Crop α	23	23	6	20	3	20
Test Accuracy	0.67	0.665	0.66	0.65	0.645	0.64
	bottle	tank	sea	rocket	orchid	palm_tree
Random Crop α	20	16	3	16	13	3
Test Accuracy	0.64	0.64	0.625	0.625	0.615	0.605
	cloud	telephone	cup	shark	whale	poppy
Random Crop α	0	30	10	86	23	13
Test Accuracy	0.595	0.595	0.595	0.59	0.58	0.575
	bridge	plate	streetcar	pickup_truck	willow_tree	maple_tree
Random Crop α	30	26	20	13	0	3
Test Accuracy	0.57	0.56	0.54	0.54	0.525	0.525
	trout	aquarium_fish	rose	worm	bicycle	lion
Random Crop α	20	20	23	10	3	6
Test Accuracy	0.52	0.515	0.51	0.505	0.505	0.5
	forest	butterfly	pear	tractor	chimpanzee	clock
Random Crop α	20	20	26	40	3	20
Test Accuracy	0.5	0.49	0.49	0.485	0.48	0.48
	leopard	beetle	tiger	raccoon	spider	pine_tree
Random Crop α	20	20	20	20	26	3
Test Accuracy	0.48	0.475	0.475	0.465	0.465	0.455
	dolphin	bee	tulip	lamp	bus	train
Random Crop α	26	3	16	13	10	20
Test Accuracy	0.455	0.455	0.44	0.44	0.435	0.435
	elephant	sweet_pepper	caterpillar	mean	table	cattle
Random Crop α	0	3	10	20	13	30
Test Accuracy	0.435	0.42	0.41	0.4098	0.405	0.395
	house	cra	wolf	mushroom	dinosaur	hamster
Random Crop α	13	3	6	3	10	6
Test Accuracy	0.395	0.39	0.39	0.385	0.38	0.38
	bed	boy	porcupine	lobster	fox	camel
Random Crop α	13	6	20	10	10	16
Test Accuracy	0.375	0.37	0.36	0.36	0.35	0.34
	flatfish	snake	kangaroo	baby	ray	couch
Random Crop α	20	26	13	6	0	3
Test Accuracy	0.34	0.335	0.335	0.325	0.32	0.315
	possum	turtle	bowl	woman	man	girl
Random Crop α	16	10	26	26	20	20
Test Accuracy	0.31	0.3	0.285	0.275	0.27	0.265
	crocodile	bear	squirrel	mouse	shrew	lizard
Random Crop α	16	20	10	6	6	3
Test Accuracy	0.255	0.255	0.25	0.245	0.24	0.235
	beaver	snail	rabbit	seal	otter	ideal

Random Crop α	10	10	0	0	26	N/A
Test Accuracy	0.22	0.215	0.2	0.2	0.125	0.47405

With Random Horizontal Flip

Random Crop α	chair	motorcycle	wardrobe	plain	skunk	road
Test Accuracy	0.845	0.83	0.795	0.79	0.77	0.77
Random Crop α	apple	sunflower	orange	sea	palm_tree	keyboard
Test Accuracy	0.74	0.74	0.74	0.7	0.695	0.695
Random Crop α	bottle	mountain	oak_tree	lawn_mower	skyscraper	orchid
Test Accuracy	0.685	0.68	0.68	0.675	0.675	0.665
Random Crop α	television	cockroach	tank	castle	can	cup
Test Accuracy	0.665	0.665	0.665	0.655	0.65	0.635
Random Crop α	plate	bicycle	streetcar	bridge	whale	rocket
Test Accuracy	0.625	0.625	0.625	0.62	0.615	0.615
Random Crop α	poppy	pickup_truck	rose	pine_tree	tractor	maple_tree
Test Accuracy	0.6	0.59	0.585	0.58	0.58	0.58
Random Crop α	trout	telephone	cloud	aquarium_fish	butterfly	pear
Test Accuracy	0.575	0.57	0.57	0.57	0.565	0.56
Random Crop α	worm	bee	leopard	caterpillar	raccoon	beetle
Test Accuracy	0.56	0.55	0.535	0.53	0.53	0.525
Random Crop α	train	forest	sweet_pepper	spider	shark	chimpanzee
Test Accuracy	0.51	0.505	0.505	0.495	0.495	0.48
Random Crop α	tulip	cra	wolf	dolphin	house	lamp
Test Accuracy	0.475	0.475	0.465	0.46	0.455	0.455
Random Crop α	tiger	clock	camel	mean	bus	elephant
Test Accuracy	0.45	0.445	0.44	0.4348	0.425	0.42
Random Crop α	table	snake	lion	cattle	mushroom	flatfish
Test Accuracy	0.415	0.415	0.41	0.405	0.405	0.39
Random Crop α	bed	hamster	boy	fox	dinosaur	bowl
Test Accuracy	0.385	0.385	0.37	0.37	0.365	0.35
Random Crop α	baby	porcupine	willow_tree	couch	kangaroo	woman
Test Accuracy	0.35	0.35	0.345	0.335	0.325	0.32
Random Crop α	possum	ray	turtle	crocodile	shrew	bear
Test Accuracy	0.3	0.295	0.295	0.285	0.285	0.285
Random Crop α	mouse	lobster	snail	girl	lizard	man
Test Accuracy	0.285	0.28	0.275	0.27	0.25	0.245
Random Crop α	beaver	squirrel	rabbit	seal	otter	ideal

Random Crop α	0	0	3	0	3	N/A
Test Accuracy	0.235	0.22	0.21	0.19	0.15	0.49985

Appendix G: Per-class and overall test set performances samples for the Fashion-MNIST + ResNet50 + Random Cropping + Random Horizontal Flip experiment

	Sandal	Bag	Trouser	Sneaker	Dress	A.Boot
R. Crop α	36%	3%	10%	3%	33%	0%
Test Accuracy	0.994	0.989	0.985	0.980	0.963	0.948
	Mean	Pullover	Coat	T-Shirt	Shirt	"Ideal" mean
R. Crop α	0%	0%	10%	0%	0%	N/A
Test Accuracy	0.912	0.877	0.860	0.848	0.762	0.920

Appendix H: Per-class and overall test set performances samples for the CIFAR-10 + ResNet50 + Random Cropping + Random Horizontal Flip experiment

	Automobile	Frog	Airplane	Horse	Ship	Truck
Best R. Crop α	16%	3%	33%	23%	10%	10%
Best Test Accuracy	0.893	0.865	0.861	0.850	0.847	0.846
	Mean	Deer	Bird	Dog	Cat	"Ideal" mean
Best R. Crop α	10%	16%	16%	16%	0%	N/A
Best Test Accuracy	0.764	0.732	0.694	0.679	0.592	0.786

Appendix I: Per-class and overall test set performances samples for the Fashion-MNIST + EfficientNetV2S + Random Cropping + Random Horizontal Flip experiment

	Sandal	Bag	Trouser	Sneaker	A.Boot	Dress
Best R. Crop α	16%	6%	3%	0%	10%	6%
Best Test Accuracy	0.995	0.987	0.984	0.978	0.954	0.938
	Mean	Pullover	Coat	T-Shirt	Shirt	"Ideal" mean
Best R. Crop α	0%	6%	16%	0%	0%	N/A
Best Test Accuracy	0.912	0.903	0.883	0.861	0.734	0.922

Appendix J: Per-class and overall test set performances samples for the Fashion-MNIST + ResNet50 + Random Cropping experiment

	Sandal	Trouser	Bag	Sneaker	Dress	A.Boot
R. Crop α	40%	3%	6%	6%	26%	6%
Test Accuracy	0.994	0.985	0.985	0.979	0.958	0.955
	Mean	T-Shirt	Pullover	Coat	Shirt	"Ideal" mean
R. Crop α	3%	0%	6%	3%	3%	N/A
Test Accuracy	0.910	0.871	0.869	0.864	0.717	0.918

Appendix K: Per-class and overall test set performances samples for the CIFAR-10 + ResNet50 + Random Cropping experiment

	Frog	Automobile	Airplane	Ship	Horse	Truck
Best R. Crop α	10%	10%	23%	10%	23%	26%
Best Test Accuracy	0.873	0.870	0.827	0.824	0.816	0.807
	Mean	Deer	Dog	Bird	Cat	"Ideal" mean
Best R. Crop α	10%	6%	20%	13%	0%	N/A
Best Test Accuracy	0.731	0.679	0.658	0.626	0.496	0.747

Appendix L: Per-class and overall test set performances samples for the Fashion-MNIST + SWIN Transformer + Random Cropping + Random Horizontal Flip experiment

	Sandal	Bag	Trouser	Sneaker	Dress	A.Boot
Best R. Crop α	60%	6%	6%	3%	30%	0%
Best Test Accuracy	0.994	0.982	0.978	0.969	0.9535	0.950
	Mean	Coat	T-Shirt	Pullover	Shirt	"Ideal" mean
Best R. Crop α	6%	10%	0%	6%	3%	N/A
Best Test Accuracy	0.901	0.867	0.863	0.860	0.746	0.915